J. MACROMOL. SCI.—PHYSICS, B40(5), 935–957 (2001)



# CRYSTALLIZATION IN PARTIALLY MOLTEN ORIENTED BLENDS OF POLYCONDENSATES AS REVEALED BY X-RAY STUDIES*

**Stoyko Fakirov,[1] Norbert Stribeck,[2†] Anton A. Apostolov,[1] Zlatan Dencev,[3] Boriana Krasteva,[1] Michel Evstatiev,[1] and Klaus Friedrich[4]**

[1]Sofia University, Laboratory on Structure and Properties of Polymers, 1126 Sofia, Bulgaria

[2]Institut für Technische und Makromolekulare Chemie, Universität Hamburg Bundesstr.45 20146 Hamburg, Germany

[3]University of Minho, Department of Polymer Engineering, 4800 Guimaraes, Portugal

[4]Institute for Composite Materials, University of Kaiserslautern, 67663 Kaiserslautern, Germany

## ABSTRACT

Oriented fibers or films of binary polymer blends from polycondensates were investigated by two–dimensional (2D) wide–angle X-ray scattering (WAXS) during the finishing process of microfibrillar reinforced composite (MFC) preparation, that is, heating to a temperature between the melting temperatures of the two components, isothermal annealing, and subsequent cooling. It is shown that the crystallization behavior in such MFC from polycondensates depends not only on the blend composition, but also on thermal treatment conditions. Poly(ethylene terephthalate)/polyamide 12 (PET/PA12), poly(butylene terephthalate)/poly(ether ester) (PBT/PEE), and PET/PA6 (polyamide 6) composites were prepared in various compositions from the components poly(ethylene terephthalate) (PET), polyamide 12 (PA12), polyamide 6 (PA6), poly(butylene terephthalate) (PBT), and poly(ether ester) (PEE). Materials were investigated using rotating anode and synchrotron X-ray source facilities. The effect of the annealing time on the expected isotropization of the lower–melting component was studied in the

*Dedicated to Prof. Francisco J. Baltá Calleja on the occasion of his 65th birthday.

†Corresponding author. E–mail: Norbert.Stribeck@desy.de

  

PET/PA6 blend. It was found that PA6 isotropization took place after 2h; shorter (up to 30 min) and longer (up to 8 h) melt annealing results in oriented crystallization due to different reasons. In PET/PA12 composites, the effect of PA12 transcrystallization with reorientation was confirmed for various blend compositions. The relative strength of the effect decreases with progressing bulk crystallization. Earlier presumed coexistence of isotropic and highly oriented crystallites of the same kind with drawn PBT/PEE blend was confirmed by WAXS from a synchrotron source.

*Key Words:* Composite; Isotropization; PET/PA6 blend; PET/PA12 blend; Poly(Butylene terephthalate); Poly(Ether ester); Transcrystallization

## INTRODUCTION

The preparation of materials with good processing and performance properties by blending different polymers requires sound scientific background. In particular, this is true if one or several components of the blend are crystallizable or can undergo chemical modifications during the mixing process, as is in the case of blends from various condensation polymers.

If chemical reactions are negligible, blending of two or more condensation homopolymers generally results in materials in which each component forms a separate phase. As a rule, the properties of the basic materials are combined, which is the characteristic feature of physical modification. Such physical blends comprising condensation polymers have been investigated and reviewed extensively during the past few decades [1]. Attention has been focused on the ability of such polymers to form homogeneous mixtures with each other as well as with a wide variety of other materials [2–4]. The beneficial properties that may be obtained by physical blending of polycondensates have been studied as well [5].

The other extreme blending process is denoted by the case in which chemical reactions play a major role. It is called *reactive blending*. Typical reactions observed are transesterification, transamidation, ester–amide exchange, etc. [6–9]. They take place at elevated temperatures, often in the presence of appropriate catalysts and have a significant effect on the mechanical properties of the blend. The said reactions result in a partial or total compatibilization of the blend constituents [8, 10]. Compatibilization may impart new properties to the material. It is worth mentioning however, that during blend production, the degree of conversion caused by the chemical reactions should be carefully monitored and kept below a characteristic threshold value. Otherwise, instead of preparing a homopolymer blend with some degree of compatibility, one may obtain a mixture of block copolymers with different block lengths in return [9].

Up to now we have only considered blends of condensation homopolymers. However, it is well known that chain orientation strongly affects the mechanical properties of polymer materials. Practical examples for blends taking advantage of orientation are fiber–reinforced composites consisting of an isotropic matrix

(polypropylene, polyamides, etc.) embedding oriented fibers (e.g. from carbon, glass, Kevlar etc.) [11,12].

During the past decade it was recognized that the mechanical characteristics of many polymers can as well be improved by means of their own morphological entities, such as fibrils, crystallites or fibers [13]. According to this concept, the reinforcing elements grow in the amorphous matrix of the polymer itself during a crystallization process. Within the last years, various types of these self–reinforced composites have been developed and studied in detail. Among them are systems produced by first blending of thermotropic liquid crystalline polymers (LCP) with some flexible commercial engineering polymers [14–16] followed by processing at high elongational flow. Under such conditions, the LCP domains are converted into dispersed and highly oriented microfibrils with a high aspect ratio serving as the reinforcing phase. Thus one deals with an in situ reinforced composite [17].

A new type of polymer–polymer composite has recently been developed [18–20] based on blends of two or more immiscible thermoplastic semicrystalline polymers with properly selected melting temperatures. They are known as *microfibrillar reinforced composites* (MFC). Their manufacturing includes three processing steps: (1) melt blending of the starting neat polymers and extrusion, (2) cold drawing of the blend, and (3) subsequent annealing of the drawn blend at constant strain and at $T_1 < T < T_2$, where $T_1$ is the melting temperature of the lower melting component and $T_2$ is that of the higher melting one.

On drawing, the components of the blend are oriented and microfibrils of both components are created. The final stage of annealing the oriented blend is essential to the formation of a MFC material. The temperature is set between the melting temperatures of the two blend components. By doing so, fusion of the lower melting polymer takes place, ultimately forming an isotropic, relaxed matrix, whereas the microfibrils of the higher melting component, their orientation, and morphology are preserved. Bundles of such aligned microfibrils finally form the reinforcing phase of the MFC [21].

Let us point out the principal differences between LCP-containing composites and MFC. First, the MFC are reinforced by microfibrils of flexible macromolecules whereas the *in situ* LCP composites have reinforcing fibrils built from rigid, rodlike molecules. Second, the LCP reinforcing elements are formed in a matrix phase environment during the extrusion stage, whereas the essential finishing step for the MFC preparation is generation of the matrix phase by annealing (isotropization). Ultimately, as far as the size of reinforcing elements is concerned, the two types of composites take an intermediate position between two extreme cases: traditional macrocomposites reinforced with glass or carbon fibers (having diameters typically of a couple of microns), on the one hand, and the molecular composites with their reinforcing elements being the single macromolecules [22], on the other. Oriented reinforcing LCP domains [17], as well as the microfibrils in MFC [21], show typical diameters from 100 to 300 nm up to 1000 nm.

As in the case of the fibrous macrocomposites [23], for the MFC it is now unambiguously established that the interactions between the microfibrils and the matrix, both physical and chemical, are of prime importance for the improvement of many of the MFC properties [18–21]. Since these interactions are particularly effective during the isotropization of one component of the oriented polymer blend, the goal of the present paper is to shed more light on this process for the case of several oriented blends of condensation polymers, which are already used or potentially useful for MFC preparation. The duration and temperature of isotropization are defined for each particular blend and therefore need to be studied more thoroughly. A further goal of this study was to investigate the peculiarities of crystallization of the MFC matrix taking place on cooling to room temperature of the partially molten blend.

The discussed transitions strongly affect the semicrystalline structure of the blend. Therefore the method of wide-angle X-ray scattering (WAXS) was employed. This method facilitates detection of crystallite orientation and perfection even in very early stages of the crystallization process. Moreover, the high flux of a synchrotron radiation source enables us to record the process of MFC formation *in situ*.

## EXPERIMENTAL

### Materials and processing

Commercial engineering grade polymers poly(ethylene terephthalate) (PET) (Vidlon, Bulgaria) (**1**), polycaprolactam (polyamide 6, PA6) (Vidamid, Bulgaria) (**2**), and polylauryllactam (polyamide 12, PA12) (Hoechst, Germany) (**3**) were dried in an oven at 120°C for 24 h. Pellets of the PET and PA6 homopolymers were melt blended in 50/50 and 40/60 weight ratios of PET/PA6. As a catalyst a small amount of *p*-toluenesulfonic acid (0.35 wt% with respect to the amount of PA6) was added. In the same way, samples with three different weight ratios (40/60, 70/30 and 85/15) of PET/PA12 were obtained by non catalyzed melt mixing, namely 60/40, 70/30 and 85/15.

Blending of the above materials was performed in a Brabender single screw lab extruder at 15–20 rpm. The extrudate from a 2 mm capillary die was immediately quenched in a water bath at 15°C. After that the strands were drawn at room temperature on a Zwick 1464 machine at a strain rate of 50 mm/min to reach a draw ratio $\lambda = 3.5 - 4.5$ and then flushed with hot air (60°C – 65°C) to remove internal stress. Finally the filaments were subjected to isothermal annealing with fixed ends for various times $t_a$ at different annealing temperatures $T_a$ in vacuum, as indicated in Table 1.

A blend of PBT (**4**) (Celanex, Celanese Corp., USA) and a poly(ether ester) (PEE) thermoplastic elastomer (**5**), which was a copolymer of PBT as hard segments and poly(ethylene glycol) (PEG) as soft segments, was also prepared as described in detail in Ref. 24. In summary, the procedure involves cooling of the

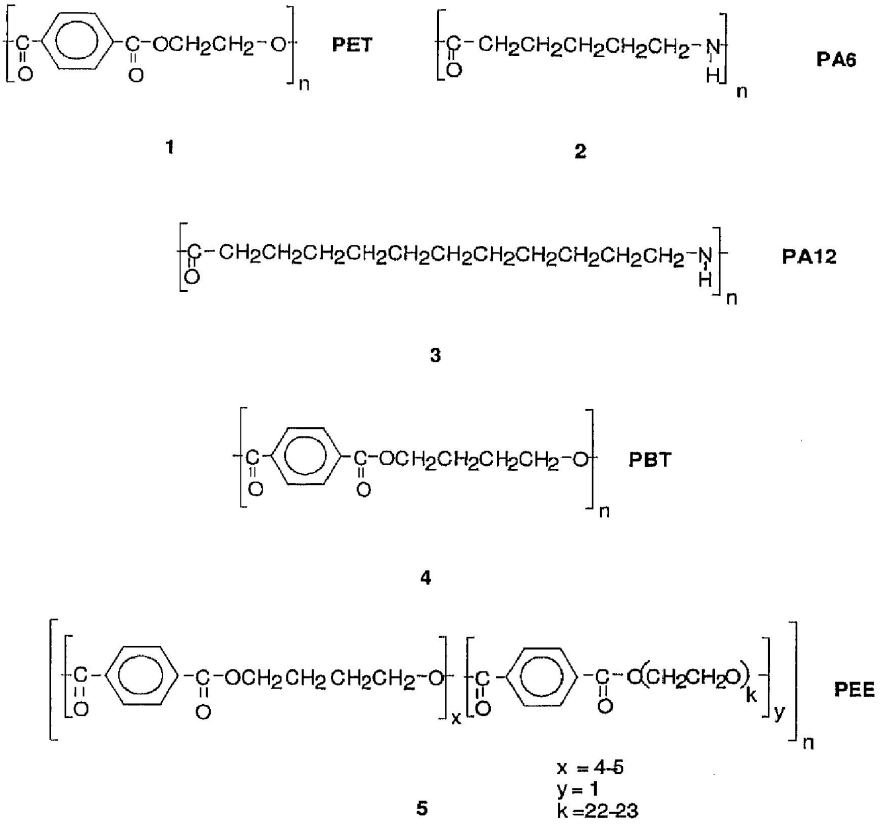


Structure 1: Commercial engineering grade polymers.

PBT and PEE polymers in liquid nitrogen and grinding them finely. The PEE employed had soft segments built from PEG with a number average molecular weight $M_n$ of 1000 g/mol; the ratio of the hard segments to the soft segments was 49 to 51 wt%. This PEE was mixed with PBT in a 51/49 weight ratio of PBT to PEE, and the resulting blend was designated as B75/25. The powder blend was dried in vacuum and subsequently used for preparation of films. These were obtained in a melt index instrument equipped with a flat die [24]. The films were drawn to $\lambda = 4.5$ at room temperature at a draw rate of 5 mm/min, followed by annealing with fixed ends at 200°C for 6 h.

### Wide–angle X–ray scattering measurements

WAXS patterns from the samples were obtained by means of different radiation sources and instrumentation. For some of the samples, patterns were recorded using synchrotron radiation, generated ad beamline A2 of HASYLAB in Hamburg, Germany. samples were mounted within a computer-controlled heating oven. The sample-to-detector distance was set at 90 cm. Most of the diffraction patterns

Table 1: Sample Preparation conditions

| Sample | Draw ratio $\lambda$ | Annealed in Vacuum with fixed ends | |
|---|---|---|---|
| | | $T_a$, °C | $t_a$, h |
| PA12 | 4 | 145 | 1 |
| PET/PA12 60/40 wt% | 4 | 220 | 12 |
| | 4 | 220 | 24 |
| | 4 | 220 | 12 |
| | 4 | 220 | 24 |
| PET/PA12 85/15 wt% | 4 | 220 | 12 |
| | 4 | 220 | 24 |
| PET/PA6 50/50 wt%[a] | 3.5 | 160 | 6 |
| | 3.5 | 220 | 4 |
| | 3.5 | 220 | 8 |
| | 3.5 | 240 | 4 |
| | 3.5 | 240 | 8 |
| PET/PA6 40/60 wt%[a] | 3.5 | 220 | 6 |
| PEE (49/51 wt%), PBT | –- | — | — |
| B75/25 | 4.5 | 170 | 6 |

For sample designation, see the text.

[a] With 0.35% *p*-toluenesulfonic acid as a catalyst for the interchange reactions

were registered by means of a two-dimensional (2D) image plate detector. In some cases, a 2D Gabriel detector was used. For several other samples, WAXS patterns were collected using a pinhole camera on an 18–kW rotating anode tube using $CuK_\alpha$ radiation, a graphite monochromator, and a 2D gas detector, with the sample-to-detector distance being set to 68 mm.

## RESULTS AND DISCUSSION

### Isotropization kinetics in oriented PET/PA6 blends

The best studied material for MFC manufacturing is the blend of PET and PA6 homopolymers [18–21,25]. As already mentioned, annealing of oriented PET/PA6 blends at temperatures above $T_m$ of PA6 but below $T_m$ of PET alters the orientation of the PA6 matrix and is essential to MFC preparation. Therefore, it appeared reasonable to record the structural changes in an oriented PET/PA6 blend during a complete annealing cycle.

In Figs. 1a–e, WAXS patterns of the sample PET/PA6 40/60 are depicted that were recorded during processing at different stages of the MFC finishing cycle: (a) before starting the process at 30°C; (b) after annealing 5 min at 240°C; (c) after 10 min annealing; (d) after 15 min (end of the annealing period), and (e) again at

30°C, after cooling the sample. The heating and cooling rates are 20°C/min and 10°C/min, respectively. All the images were taken with a 2D Gabriel detector at HASYLAB.

Fig. 1a reveals a pattern typical for a highly oriented system insofar as isointensity Debye rings are missing. The PA6 reflections are superimposed on the sharp, pointlike reflections of PET. All reflections are concentrated on or close to the equator of the pattern. Since the reflections of PA6 are not of Debye ring type, one can conclude that the complete PA6 matrix material is oriented. In the pattern taken immediately after annealing at $T_a = 240$°C for 5 min (Fig. 1b), the PA6 phase appears to be almost completely molten. The patterns obtained after longer annealing are similar (Fig. 1c, 10 min; Fig. 1d, 15 min) when also taken at $T_a = 240$°C. One observes that the PA6 reflections have been transformed into an isotropic amorphous halo.

Cooled to 30°C the composite exhibits an unexpected WAXS pattern (Fig. 1e). The PA6 reflections reappear, but not as closed Debye rings, typical for isotropic crystalline materials. Again, they exhibit the shape of clear arcs, superimposed on the equatorial PET reflections. This means that the annealing time of 15 min at a temperature higher than $T_m$ of PA6 is not sufficient to erase the orientational memory of PA6. So we decided to increase the duration considerably. To obtain higher resolution WAXS patterns, we employed an image plate detector. The recorded WAXS images are presented in Fig. 2a–f.

Fig. 2a shows the WAXS pattern of the initial drawn sample PET/PA6 40/60. The image confirms the absence of PA6 rings, thus proving the orientation of the complete polyamide matrix. The pattern in Fig. 2b was taken at $T_a$ = 200°C (heating rate of 20°C/min, exposure time 1 min) and reveals the gradual transformation of the PA6 reflections into an amorphous halo. This process appears to have been completed after some minutes (Figs. 1b–1d), but in the present case, a longer annealing (2 h at 240°C) was applied to check if the subsequent crystallization will take place in the oriented state (as Fig. 2e shows). The next image (Fig. 2c) was taken at 240°C after this longer annealing.

At 100°C, during sample cooling at 10°C/min, the pattern shown in Fig.2d was recorded. One observes crystallization of the PA6 phase, but despite the prolonged annealing period it is not isotropic either. Closer visual inspection reveals that the apparent Debye rings, in fact, represent very long arcs with only decreased intensity about the meridian. For this material, isotropic Debye rings were only observed after heating to 280°C (Fig. 2e), annealing for 10 min, and subsequent cooling to room temperature at 10°C/min (Fig. 2f). By the way, the same things happened with the PET (Fig. 2f).

These results are a valuable extension of previous ones in which short melt annealing times were studied. They demonstrate that even 2 h annealing of the melt cannot prevent the PA6 phase from crystallizing with some orientation. Comparison of Figs. 2a and 2d reveals that the length of the arcs of PA6 in the second

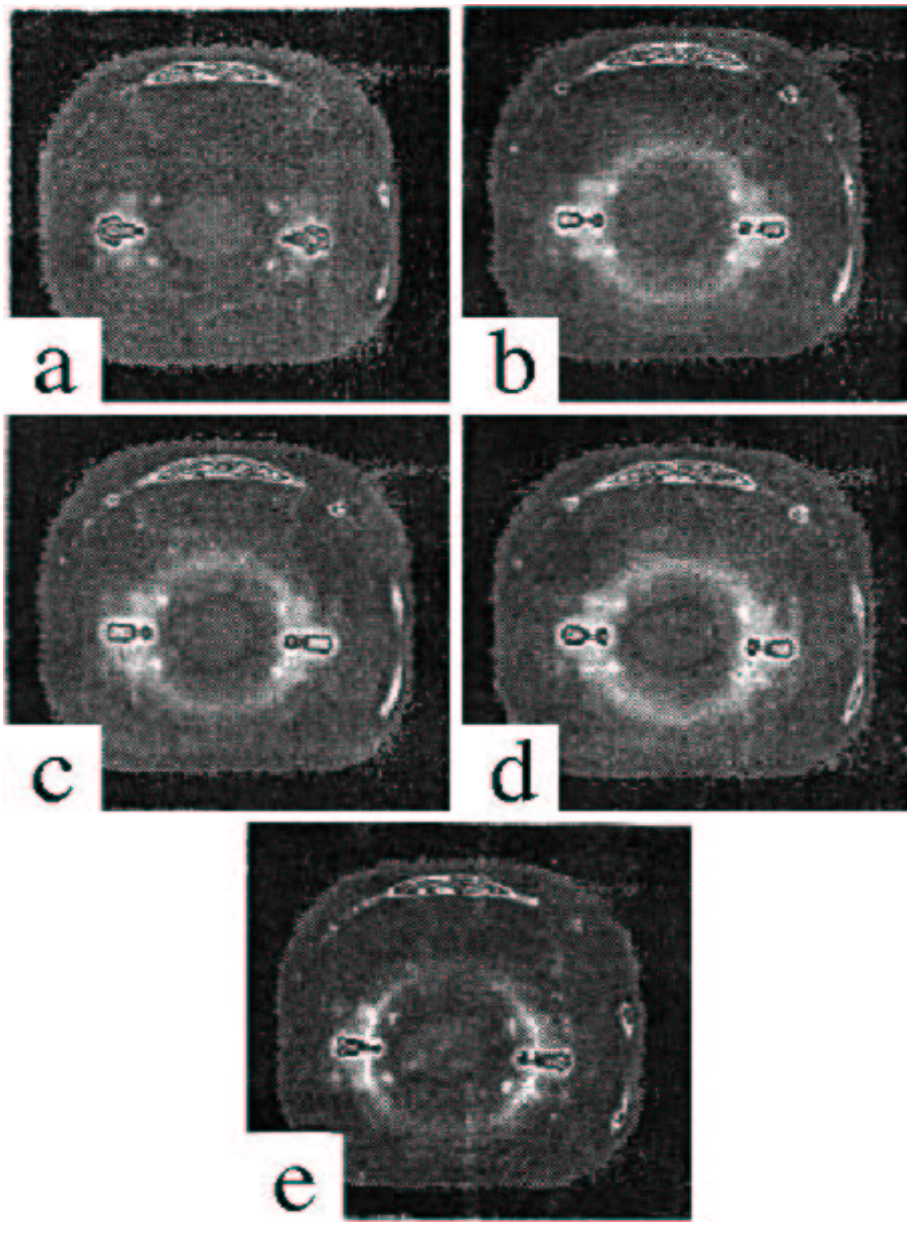


Figure 1: WAXS patterns of blend PET/PA6 40/60 wt% during an annealing cycle. Images taken at the indicated temperatures by means of synchrotron radiation and a 2D Gabriel detector: (a) at 30°C, starting sample (oriented and annealed for 4 h at 220°C); (b) after 5 min annealing at 240°C; (c) after 10 min annealing at 240°C; (d) after 15 min annealing at 240°C; and (e) again at 30°C after cooling the sample from 240°C. Heating and cooling rates were 20°C/min and 10°C/min, respectively.

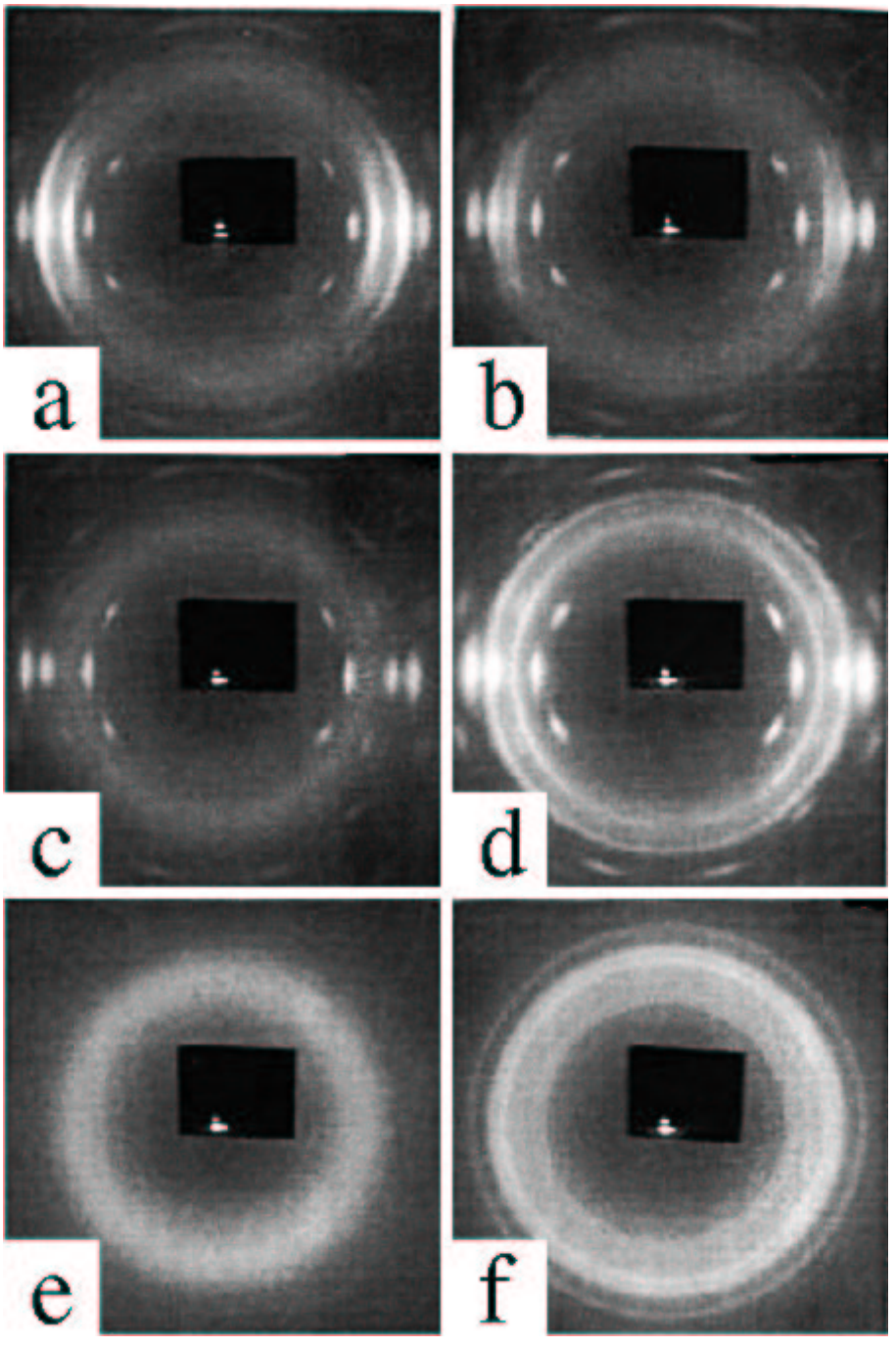


Figure 2: WAXS of blend PET/PA6 40/60 wt% during prolonged annealing. Patterns from synchrotron radiation source recorded on an image plate at the indicated temperatures: (a) at room temperature of the starting sample (oriented and annealed for 4 h at 220°C); (b) during heating (20°C/min) at 200°C; (c) after 2 h annealing at 240°C; (d) during cooling (10°C/min) at 100°C (after 2 h annealing at 240°C); (e) at 280°C when reheated; and (f) at room temperature after heating to 280°C, annealing for 10 min, and subsequent cooling (10°C/min).

pattern is much longer. Now, the question is whether this oriented crystallization (Fig. 1e and Fig. 2d) is caused by information remnant in the PA6 chain conformation itself (memory effect) or if it is induced by the PET phase (transcrystallization). Obviously, the oriented crystallization should be discussed bearing in mind the ability of PA6 moieties to establish hydrogen bonds with each other, as well as with the PET from the embedded reinforcing fibrils. This point is discussed in the section in which the results obtained with PET/PA12 blends are presented.

Memory effect in polymers, more specifically the so-called orientational memory in the molten state, was studied earlier by Keller and Marchin [26] and more recently by Khanna and Reimschussel [27]. In their studies on some neat polymers employing mostly differential scanning calorimetry (DSC) and light microscopy, Khanna and Reimschussel pointed out that the crystallization behavior of polymers from the molten state is strongly influenced by the orientational history. The present studies on an oriented and annealed PET/PA6 blend demonstrate a similar phenomenon that should be taken into account when properties of PET/PA6 microfibrillar composites are discussed. Furthermore, one should also consider the possible ability of the strongly oriented PET phase to promote PA6 orientational crystallization even after erasing the orientational memory. The occurrence of interchange chemical reactions between the molten PA6 and the PET amorphous regions [28] could also have some impact on the oriented crystallization of PA6 because chemical links generated between PET and PA6 drastically hinder disorientation of molten PA6 close to the domain boundary. These and other aspects of the problem are currently under more detailed investigation, and the results will be reported separately.

### Coexistence of Two Chemically and Crystallographically Identical Populations of Crystallites in the Oriented and Isotropic State

It is well known that crystallites of two chemically different polymers may coexist in blends [29]. The studied case of the PET/PA6 blend is such an example [18–21,25]. It has to be considered a different case, however, if an oriented population of crystallites can coexists with an isotropic one. For a couple of systems, including PET and some polyamides, the feasibility has been proven, as is demonstrated for the case PET/PA6 (Figs. 1 and 2) above. Here, the coexistence of differently oriented crystallites is promoted by a chemical difference.

Let us now discuss if different populations of crystallites of one and the same polymer can coexist, which can be distinguished by different degree of orientation. Again, it is convenient to start from a two–component blend comprising crystallites with different melting temperatures, but the same chemical composition. If this condition can be maintained throughout a straining process that is aligning both components, MFC formation may be initiated by subsequent annealing of the drawn blend between the melting temperatures of the two crystallite populations. The facility for generating two populations of crystallites from the same kind of

polymer that melt at different temperatures is well understood. It is based on the substantial increase of melting temperature as a function of increasing crystallite size and perfection. Thus, it should be possible to transform small and imperfect crystals from the oriented to the isotropic state by sufficiently long melt annealing (cf. Figs. 1 and 2).

In a recent study on homo-PBT blended with a poly(ether ester) based on PBT and poly(tetramethylene glycol), Gallagher et al. [30] observed cocrystallization of PBT moieties arising from both the homo– and copolymer under all crystallization conditions studied. For their samples, with a PBT content in the PEE between 75 to 91 wt% a special type of cocrystallization was observed. It is characterized by the same crystallite containing both kinds of PBT moieties.

We have investigated a similar blend, containing a poly(ether ester) with soft segments based on poly(ethylene glycol) [24,31] and a much lower PBT content ( 49 or 75 wt%). the blend was drawn and subsequently annealed at a temperature between the melting temperatures of PEE (191°C) and a homo-PBT (226°C). During annealing, disorientation took place. We did not observe the mentioned type of cocrystallization, but quite the opposite — formation of continuous crystals comprising two, possibly nonspatially separated (i.e., having common crystal surfaces), crystallographically identical populations of crystallites, differing in size, perfection, origin and time of appearance [24]. This phenomenon was originally [24] called "partial cocrystallization" and proven by small-angle X-ray scattering (SAXS) [24], DSC [24], and microhardness measurements [32]. Thermograms of the oriented blend show two melting peaks, thus proving that the blend comprises two populations of crystallites, probably the more perfect ones arising from the homopolymer PBT and the less-prefect crystallites made from the PBT blocks of the PEE block copolymer [24]. In the SAXS curves of such a blend, for example, a maximum comprising two overlapping peaks positioned at different scattering angles $2\theta$ was observed, and measurements carried out during sample heating showed that one of these two peaks disappears close to the lower melting temperature, whereas the other peak vanishes above the higher melting temperature (as determined from DSC). This is an implicit indication of the coexistence of two types of PBT crystallites differing in perfection and spatial arrangement [24].

The coexistence of two types of crystallographically identical PBT crystallites in the blend, which can be distinguished by their degree of perfection was also proven by microhardness measurements. It is known that PBT crystals undergo a polymorphic alpha-beta transition on stretching at a certain external deformation. This transition may be registered by microhardness measurements since the two crystalline modifications of PBT have different density and different microhardness. In the case of the first type of cocrystallization, as reported by Gallagher et al. [30] for their system, only a single population of crystallites would exist, and consequently only one polymorphic transition would be found with the progress of deformation. Recently, we registered two distinct polymorphic alpha-beta tran-

sitions of PBT in the microhardness versus external deformation dependencies for the PBT/PEE blend with lower PBT content [32]. It was concluded that homo-PBT and the PBT segments from PEE segregate in different crystallites [32].

A clear support for the occurrence of segregated crystallization was found in a series of 2D WAXS flat-film patterns taken at room temperature after different thermal treatment of the predrawn blend [24]. The WAXS pattern of a sample annealed at a relatively low temperature of 170°C (i.e., below the melting temperature of the crystallites arising from both the homo-PBT and the PBT from PEE) showed that all PBT crystallites are highly oriented. On the contrary, the X-ray pattern of the sample after annealing at 200°C, that is, between the melting temperatures of the homo-PBT crystallites ($T_m = 226$°C according to DSC measurements [24]) and that of PBT in PEE ($T_m = 191$°C [24]) contained reflections of both PBT crystals in highly oriented state, as well as reflections of randomly oriented PBT crystals originating from the PEE component.

Since the observed coexistence of chemically and crystallographically identical crystallites in the oriented and isotropic states appeared rather uncommon, the same blend was again investigated, now utilizing radiation from a synchrotron source. The sample was heated stepwise from 95°C up to 210°C, held at constant temperature for 1 h, subsequently cooled to 95°C, held for 5 min, again heated to 230°C, and cooled to 95°C. The heating and cooling rate was 10°C/min. WAXS patterns were recorded on an image plate and exposed for 1 min every 5 min. Three selected patterns are shown in Fig. 3.

Fig. 3a shows a pattern taken at 130°C from the initial sample of the drawn blend, annealed at 170°C. Sharp reflections of oriented PBT superimposed on a faint amorphous halo are observed in this picture.

Fig. 3b shows a pattern taken from the sample at 95°C after isothermal annealing at 210°C. Sharp reflections of the oriented homo–PBT crystallites superimposed on weak but clear isotropic Debye rings of randomly oriented PBT from PEE are found in this image. The crystallites of PBT in PEE were molten at 210°C and recrystallized thereafter, but without preferred orientation. The amorphous halo now is more pronounced than in the previously discussed image (Fig. 3a) due to the poorer crystallization conditions (nonisothermal crystallization, in contrast to the earlier experiments [24]), leading to a lowered degree of crystallinity.

Thus, by performing several properly chosen steps with respect to melting point and orientation, a common blend of PBT and PEE was transformed into a peculiar material in which two chemically and crystallographically identical populations of crystallites are coexisting. Although both populations are crystallographically identical, they differ in orientation, perfection and melting temperature. Here the main reason for the creation of imperfect crystallites is the short block length of the PEE hard segments. It was shown in an earlier study [33] that for the PEE with 49 wt. % PBT, the hard segments are generally shorter than the equilibrium thermodynamic lamella thickness for common crystallization temperatures.

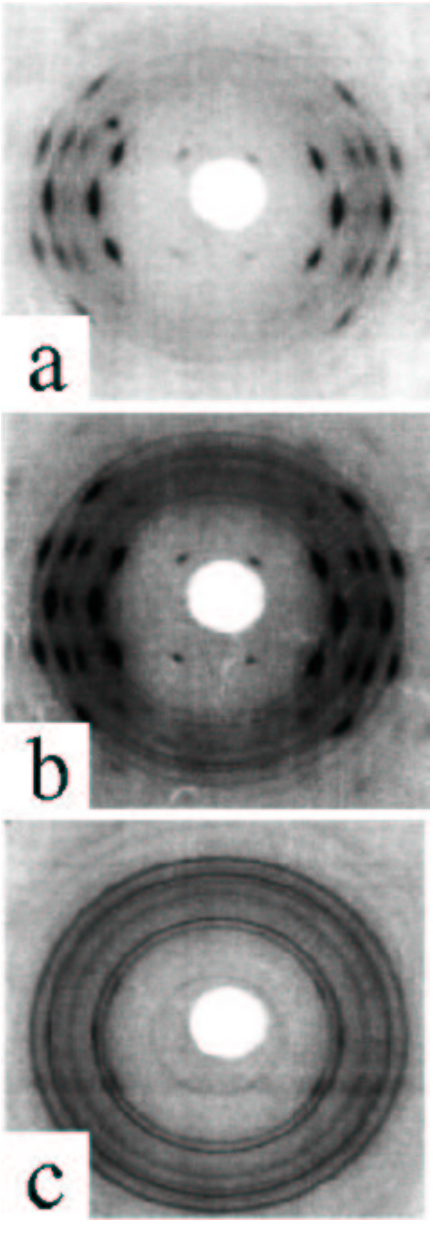


Figure 3: WAXS of sample B75/25 during heat treatment. Patterns recorded at the indicated temperatures on an image plate using a synchrotron source: (a) during heating at 130°C; (b) during cooling at 95°C (after isothermal annealing for 1 h at 210°C); (c) during cooling at 95°C (after heating to 230°C at 10°C/min, isothermal annealing for 5 min, and subsequent cooling at 20°C/min).

Finally, after heating to 230°C and subsequent cooling (Fig. 3c) sharp Debye rings of randomly oriented PBT crystallites are observed, showing that almost all of the PBT crystallites were molten and recrystallized isotropically. Only some very perfect PBT crystallites appear not to have been molten and contribute to some weak pointlike reflections, as can be seen in this figure.

In summary, two types of cocrystallization can occur in a polymer blend when there is a common crystallizable component. Either the formed crystallites contain an intimate mixture of chain segments from both the homopolymer and the copolymer, or there is segregation, and regions with enriched/depleted homopolymer content can be distinguished. We already considered two blends from PBT with different kinds of PEE. Similarly, it is possible to continue the variation of blend composition by exchanging the soft segment block of the PEE or its hard segment block in relation with the homopolyester. Blends from polyamides with poly(ether ester amide)s based on the same polyamide and poly(ethylene oxide) [34] are promising candidates for investigation of the cocrystallization phenomenon as well. Such studies are in progress.

## Transcrystallization with Change of Orientation in Poly(Ethylene terephthalate)/Polyamide Blends

A special case of crystallization in fiber reinforced composites is transcrystallization [35]. It may only be found, if heterogeneous nucleation at the surface of the reinforcing fiber is a primary process and the resulting crystal growth is restricted to the lateral direction, enforcing a columnar layer to be generated in the polymer matrix around the fiber. Such a transcrystalline region around the embedded fibers is thought to be of prime importance to the improvement of the adhesion between the fibers and the matrix, and thus is expected strongly to affect the properties of the composite. Important parameters controlling the development of the transcrystalline zone are the nucleating activity of the fiber surface and the crystallization kinetics of the matrix material.

As recently summarized by Chen and Hsiao [36], the fiber surface tends to cause nucleation of the matrix under the following conditions: (1) a topographical match between fiber and matrix; (2) a thermal conductivity mismatch between fiber and matrix; (3) an extensional flow field induced by processing conditions, or (4) high surface free energy on the fiber. Depending on the mechanism involved, different cases of mutual rearrangement of the polymer chains in the reinforcing fibers and the surrounding matrix are reported. For instance, in composites from cellulose and polypropylene (PP), the chains of PP align parallel to the fiber axis (FA) in the transcrystalline zone [37]. The same alignment prevails in some advanced polymer composites based on PEKK and PEEK reinforced by carbon, Kevlar, or glass fibers [36].

In a detailed study on interfacial interaction between Kevlar filaments in a PA6 matrix that was crystallized from the melt, two kinds of transcrystalline zones were

observed around the filament surface [38]. It was confirmed by polarized light microscopy, microbeam X-ray diffraction, and transmission electron microscopy that the PA6 macromolecules crystallize epitaxially. The a*- and a-axes of PA6 are directed along the radius of the Kevlar filament in the interfacial and intermediate zones, respectively. The b-axis (molecular axis) and the c-axis rotate around the a*- or a-axis [38].

In a more recent study [39] on aramid and carbon fiber reinforced polyamide 66 composites, atomic force microscopy revealed radial regularity in the transcrystalline layer relative to the fiber, and X-ray investigations of the isolated layer suggested that the macromolecules are predominantly oriented with their axis perpendicular to the fiber axis.

It should be emphasized that, to the best of our knowledge, there are no other studies, except that of ours [40], reporting chain orientation flip in one component of uniaxially oriented blends initiated by partial melting and recrystallization. We studied the transcrystallization behavior of PA12 in a blend PET/PA12 (60/40 wt%) by means of WAXS utilizing a synchrotron radiation source. It was found that the transcrystallization of PA12 during cooling of the molten PA12 in the blend is characterized by reorientation of PA12 chain axis by $90^{o}$ with respect to the PET chain axis and to the previous orientation of the PA12 chain axis itself. It was concluded that the PET microfibrils are not only effective nuclei for transcrystallization of PA12 molecules, but also cause their reorientation by $90^{o}$ with respect to their initial direction. It was noticed that the clarity of the reorientation effect in the pattern weakens during progress of the experiment. This observation was attributed to a masking effect caused from a slowly emerging isotropic ensemble of PA12 crystallites generated away from the PET microfibrils. In order to study this complex process more deeply, three different compositions of this blend (60/40, 70/30 and 85/15 wt%, cf. Table 1) have now been investigated after different durations (12 h and 24 h) of thermal treatment at a temperature of $220^{o}$C, that is, between $T_{\mathrm{m}}(\mathrm{PA12}) = 180^{o}$C and $T_{\mathrm{m}}(\mathrm{PET}) = 265^{o}$C.

The pattern in Fig. 4a originates from a cold-drawn PET/PA12 sample (60/40 wt%) annealed for 1h at $145^{o}$C, that is, prior to MFC finishing by annealing. One observes considerable orientation. Judging from the fact that all the strong reflections are placed around the equator of the pattern, one may conclude that both PET and PA12 blend constituents are aligned with their chain axes parallel to the FA. Relatively poor crystallinity is observed. The other WAXS patterns in the figure (Figs. 4b–4g) were obtained from three PET/PA12 blends after different durations of annealing. They were taken at room temperature using a rotating-anode X-ray source.

As compared to the pattern in Fig. 4a, the 2D WAXS patterns change considerably after thermal treatment at $220^{o}$C for 12 h and 24 h (Figs. 4b, 4d, 4f and Figs. 4c, 4e, 4g, respectively). While the principal alignment of the PET chains in the crystallites parallel to the drawing direction remains unchanged, the orientation of the PA12 crystallites appears neither preserved nor extinguished. Instead, the PA12

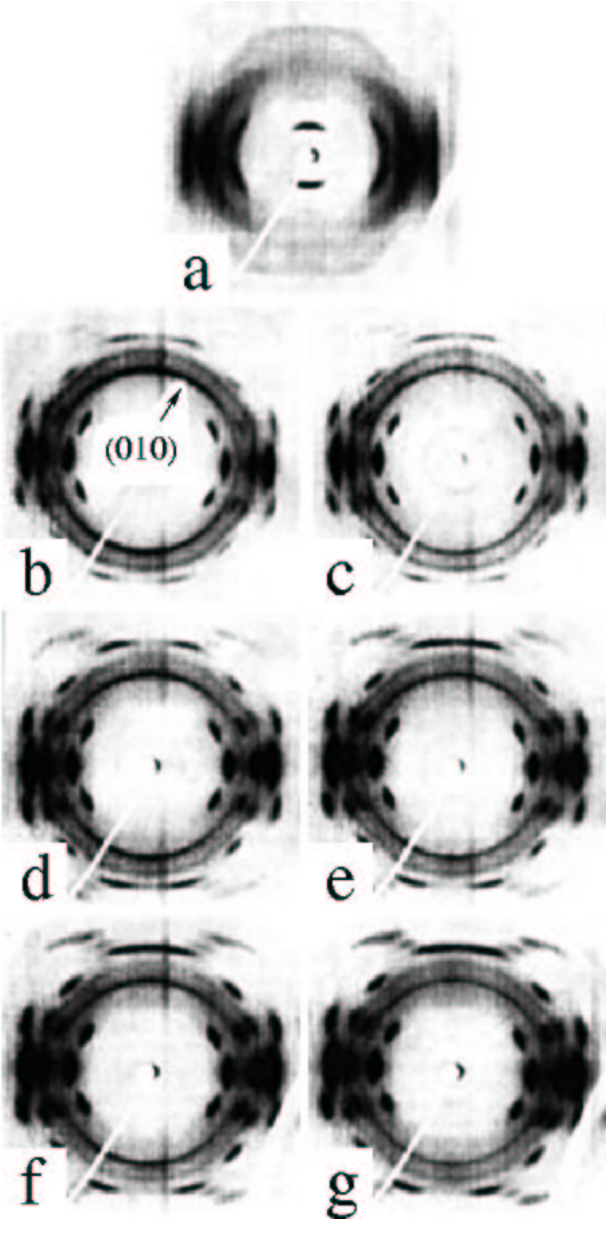


Figure 4: WAXS of different PET/PA12 blends at room temperature. Patterns recorded using a rotating anode source and a 2D gas detector: (a) sample 60/40 wt% annealed at 145°C for 1 h. The following patterns are from three PET/PA12 blends of indicated composition annealed at 220°C for indicated periods of time: (b) 60/40, 12 h; (c) 60/40, 24 h; (d) 70/30, 12 h; (e) 70/30, 24 h; (f) 85/15, 24 h; (g) 85/15, 24 h. In Fig. 4b, the position of the PA12 (010) reflection is marked.

reflections of the blends show some orientation in a direction perpendicular to the original one regardless of the polyamide content or the duration of the thermal treatment.

A more precise inspection of the scattering patterns from Fig. 4 and particularly of 3D representations of the WAXS patterns after annealing (cf. Fig. 5a) leads to the following model concerning the disposition of the PA12 chains in the crystallites with respect to the PET chain axis. Fig. 5b displays a sketch of those crystals, which show the strong reorientation effect of the (010)–reflection. Here the hydrogen–bonded planes are more or less parallel to the fiber cross section. On the other hand, the (200)–reflection is caused from PA12 crystallites, in which the hydrogen–bonded planes are stacked "from front to back" (Fig. 5c). The reflection appears to be isotropic, but some orientational memory cannot be excluded for these crystals, because a corresponding anisotropy would be hidden beneath the strong PET reflections.

Now let us return to the PET/PA6 oriented blend after conversion to an MFC by annealing. In contrast to the perpendicular orientation of polyamide chains with respect to the PET fibrils in the PET/PA12 composites, here the PA6 chains are aligned in parallel to the PET chains, as indicated by the experimental results (Figs. 1 and 2). This substantial difference in the behavior of the two polyamides, PA12 and PA6, stimulated additional investigation on the blend PET/PA6 concerning, for instance, the effect of heat treatment temperature and duration. This was done for the 50/50 wt% PET/PA6 blend, and the results of the measurements are shown in Fig. 6a–e. The first picture (Fig. 6a) originates from the drawn blend after annealing at 160°C for 6 h. The reflections of PA6 superimpose on those of the other phase (PET), with all reflections concentrated close to the equator. Annealing at 220°C for 4 h results in a different pattern; now the PET reflections are clearly observable and characteristic for a crystalline polymer in highly oriented state (Fig. 6b). The PA6 reflections, however, exhibit isointensity Debye rings, typical for unoriented crystalline materials. Longer annealing at the same temperature (8 h/220°C) and cooling to room temperature (Fig. 6c) causes two effects: (1) the original isointensity PA6 rings (Fig. 6b) become more arclike with their maximum about the equator (Fig. 6c), that is, there is a trend toward orientation of the PA6 and PET chains parallel to the fiber direction (FA); (2) additional PA6 reflection arcs emerge with their center placed on the meridian (Fig. 6c). The patterns for the sample annealed at 240°C for 4 h and 8 h (Figs. 6d and 6e, respectively) do not display any significant difference, as far as intensity increase in meridional direction is concerned. However, they undoubtedly show arc-shaped PA6 reflections that are a clear indication of PA6 orientation partially restored parallel to the PET fibrils. Comparing Figs. 6b and 6e, there is a suggestion that the higher the annealing temperature and the longer the heat treatment, the more diffuse is PA6 orientation as a result of the crystallization after PA6 melting.

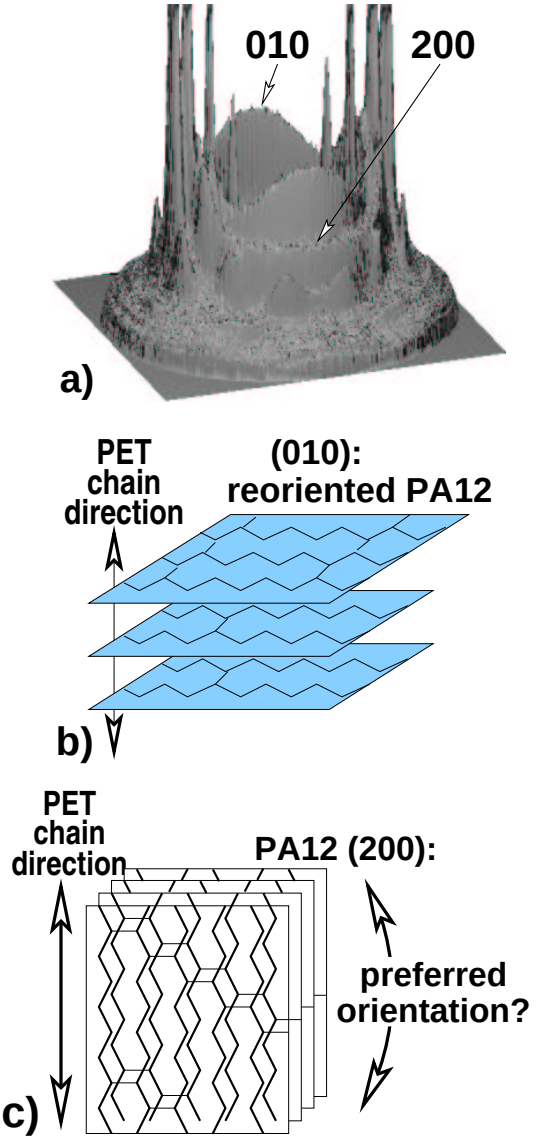


Figure 5: The 3D WAXS pattern of PET/PA12 blend and schematic representation of the mutual displacement of PET chains and PA12 chains in the transcrystalline layers after melting of PA12 and repeated crystallization as derived from the WAXS patterns displayed in Fig. 4 and in Ref. 40. (a) 3D WAXS pattern taken at room temperature after annealing for 12 h at 220°C of drawn PET/PA12 blend. The crystalline PA12 in the PET/PA12 composite is identified by its two strong reflections, (010) and (200). Meridian runs "from front to back." (b) Model derived from (010) reflection; c) Model derived from the (200) reflection.

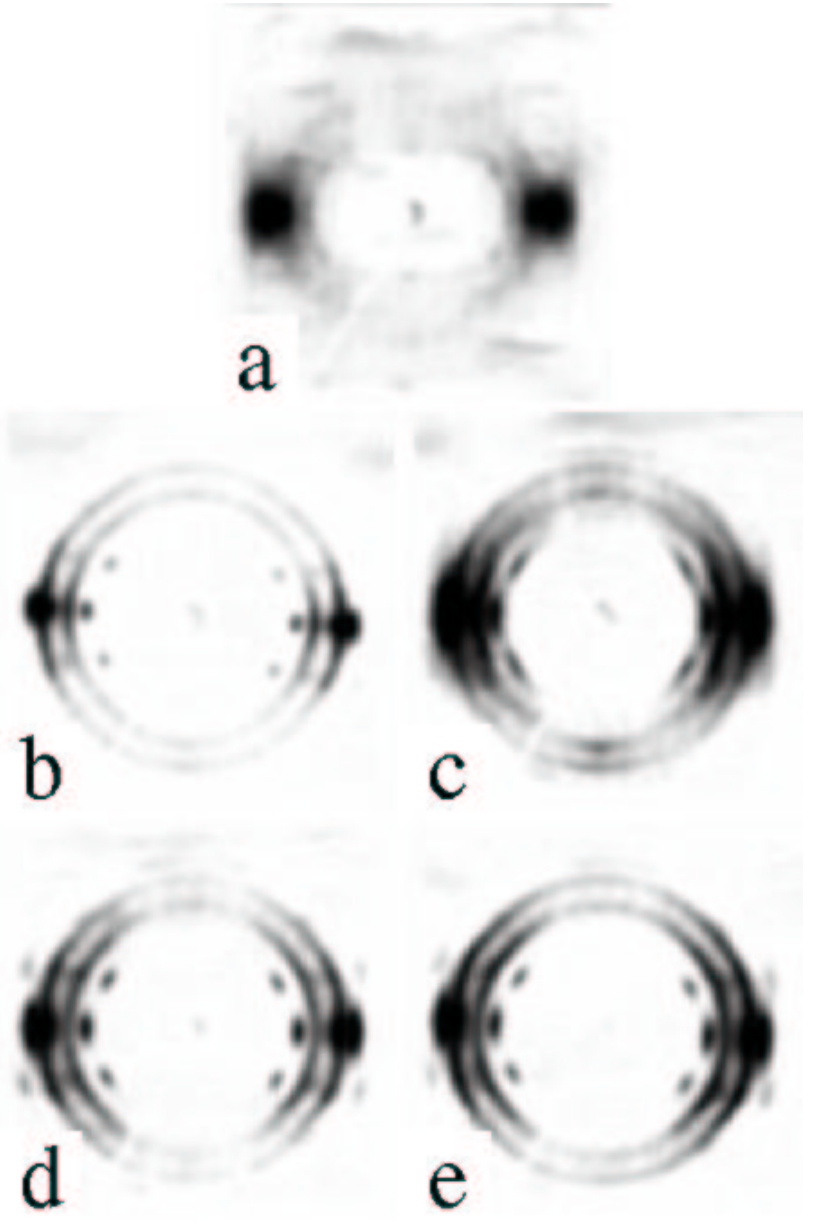


Figure 6: WAXS patterns from drawn PET/PA6 50/50 wt% blend taken at room temperature after different thermal treatment (rotating anode source, 2D gas detector): (a) 6 h at 160°C; (b) 4 h at 220°C; (c) 8 h at 220°C; (d) 4 h at 240°C; and (e) 8 h at 240°C.

Now, let us summarize the results on the predrawn binary PET/PA6 blend. The crystallization behavior of the lower melting component in the MFC finishing step depends not only on the chemical composition of the blend, but also on the treatment conditions. For instance, after very short melt annealing (up to 15 min), the PET/PA6 blend shows a tendency toward crystallization in anisotropic state (Fig. 1e), whereas 2 h melt annealing results in a more or less isotropic state at room temperature (Fig. 2d); thus, we assume that, before starting to cool the PA6 melt, it should have been more or less isotropic as well. The other extreme case is the relative long melt annealing (8 h) after which PA6 crystallizes in oriented state, returning to its initial orientation (draw direction; Fig. 6e). Obviously, this tendency is predominantly related to the advanced stage of interchange reactions between PA6 and PET during melt annealing at 240°C, as repeatedly reported [9]. The chemical bonds generated between matrix polymer and chains from the embedded microfibrils imprint an alignment of the melt (i.e., enhance the crystallization in the oriented state).

## CONCLUSIONS

The effect of transcrystallization with reorientation of PA12 in the blend PET/PA12 was firmly established for various blend compositions. It is more clearly expressed for the higher PA12 content and for shorter melt annealing time. A special polymer blend based on PBT and PEE has been developed in which two chemically and crystallographically identical populations of crystallites, differing in orientation, perfection, time of appearance, and melting temperature coexist in oriented and isotropic states. Finally, for the blend PET/PA6, it was established that short melt annealing (up to 15 min) leads to oriented crystallization; longer annealing (2 h) leads to a tendency toward PA6 crystallization in a more or less isotropic state, whereas for much longer melt annealing times (4–8 h) oriented crystallization of PA6 predominates. This crystallization in the oriented state is suggested to be stimulated by interchange reactions between the PET microfibrils and the PA6 matrix.

## ACKNOWLEDGMENT

This study was supported by the Bilateral Cooperation Program between the University of Hamburg, Germany, and the University of Sofia, Bulgaria, funded by the DAAD (German Academic Exchange Service). WAXS investigations were supported by HASYLAB, Hamburg, Germany. The partial financial support of the Deutsche Forschungsgemeinschaft (DFG FR 675/21–2) is also acknowledged. One of us (S.F.) expresses his gratitude to the Alexander von Humboldt Foundation for the Humboldt Research Award, which enabled his stay at the Institute of Composite Materials Limited at the University of Kaiserslautern, Kaiserslautern, Germany where this paper was finalized. The hospitality of the institute is also greatly appreciated.

## REFERENCES


1. Ellis, T.S. Phase Behaviour of Blends of Polyesters and Polycarbonates. Polymer. **1998**, *39* (20), 4741–4749.
2. Kollodge, J.S.; Porter, R.S. Phase Behavior and Transreaction Studies of Model Polyester/Bisphenol-A Polycarbonate Blends. I: Synthesis, End-Capping, and Characterization of Poly(2–ethyl–2–methylpropylene Terephthalate). Macromolecules. **1995**, *28* (12), 4089–4096.
3. Kollodge, J.S.; Porter, R.S. Phase Behavior and Transreaction Studies of Model Polyester/Bisphenol-A Polycarbonate Blends. II: Molecular Weight, Composition, and End–Group Effects. Macromolecules. **1995**, *28* (12), 4097–4105.
4. Rodriguez, J.L.; Eguizabal, J.I.; Nazabal, J. Phase Behavior and Interchange Reactions in Poly(butylene Terephthalate)/Poly(ester–carbonate) Blends. Polym. J. **1996**, *28* (6), 501–506.
5. Land, H.T.; Heitz, W.; Karbach, A.; Pielartzik, H. Influence of Intermolecular Interactions on Phase Behaviour and Miscibility of *para*-Linked Aromatic Polyester with Polycarbonate and Mechanical Properties of Blends. Makromol. Chem. **1992**, *193* (10), 2571–2580.
6. Brown, S.B. Compatibilization of Immiscible Polymer Blends. in *Reactive Extrusion: Principles and Practice*; Xanthos, M., Ed.; Carl Hanser Verlag: Munich, New York, 1992; 130.
7. Eersels, K.L.L.; Aerds, A.M.; Groeninckx, G. Transamidation in Melt-Mixed Aliphatic and Aromatic Polyamides. II: Molecular Characterization of PA 46/PA 6i Blends as a Function of the Extrusion Time, Extrusion Temperature, and Blend Composition. Macromolecules. **1996**, *29* (3), 1046–1050.
8. Porter, R.S.; Wang, L. Compatibility and Transesterification in Binary Polymer Blends. Polymer. **1992**, *33* (10), 2019–2030.
9. Fakirov, S., Ed. *Transreactions in Condensation Polymers*, Wiley–VCH: Weinheim, 1999.
10. Paul, D.R.; Barlow, J.W.; Keskkula, H. in *Encyclopedia of Polymer Science and Engineering*; Mark, H.F.; Bikales, N.M.; Overberger, C.G. Menges G., Eds.; John Wiley: New York, 1989; Vol. 12, 399.
11. Yu, Z.; Ait-Kadi, A.; Brisson, J. Nylon/Kevlar Composites. II. Investigation of Interfaces. Polym. Eng. Sci. **1991**, *31* (16), 1228–1232.
12. Arvanitoyannis, I.; Psomiadou, E.; Yamamoto N.; Blanshard, J.M.V. Composites of Novel Biodegradable Copolyamides Based on Adipic Acid, 1,6-Hexane Diamine and l-Proline with Short e-Glass Fibres. I. Preparation and Properties. Polymer. **1995**, *36* (3), 493–503.
13. Petermann, J.On the Plastic Deformation of Fibre Self-Reinforced Polymers. J. Mater. Sci. **1987**, *22*, 1120–1126.
14. Wei, K.H.; Su, K.F. A Study on Blends of Liquid Crystalline Copolyesters with Polycarbonate. II. Transesterification Control. J. Appl. Polym. Sci. **1996**, *59* (5), 787–796.

15. Brostow, W.; Hess, M.; Lopez, B. L.; Sterzynski, T. Blends of a Longitudinal Polymer Liquid Crystal with Polycarbonate: Relation of the Phase Diagram to Mechanical Properties. Polymer. **1996**, *37* (9) 1551–1560.
16. Chang, J.H.; Jo, B.Y.; Jin, J.I. Blends of thermotropic Liquid Crystalline Polyesters and Poly(butylene Terephthalate): Thermal, Mechanical, and Morphological Properties. Polym. Eng. Sci. **1995**, *35* (20), 1605–1614.
17. Baird, D.G.; McLeod, M.A. Liquid Crystalline Polymer Blends. In *Polymer Blends, Vol. 2 Performance*; Paul D.R.; Bucknall, C.B. Eds.; John Wiley and Sons, Inc.: New York, 2000, 429.
18. Evstatiev, M.; Fakirov, S. Microfibrillar Reinforcement of Polymer Blends. Polymer. **1992**, *33* (4), 877–880.
19. Fakirov, S.; Evstatiev, M.; Schultz, J.M. Microfibrillar Reinforced Composite from Drawn Poly(ethylene Terephthalate)/Nylon-6 Blend. Polymer. **1993**, *34* (22), 4669–4679.
20. Evstatiev, M.; Fakirov, S.; Friedrich, K. Effect of Blend Composition on the Morphology and Mechanical Properties of Microfibrillar Composites. Appl. Compos. Mater. **1995**, *2* , 93.
21. Evstatiev, M.; Nikolov, N.; Fakirov, S. Morphology of Microfibrillar Reinforced Composites PET/PA6 Blend. Polymer **1996**, *37* (20), 4455–4463.
22. Seufert, M.; Fakirov, C.; Wegner, G. Ultrathin Membranes of Molecularly Reinforced Liquids on Porous Substrates. Adv. Mater. **1995**, *7*, (1), 52–55.
23. Peacock, J.A.; Fife, B.; Nield, E.; Barlow, C.Y. A Fibre-Matrix Interface Study of Some Experimental PEEK/Carbon-Fibre Composites. In *Composite Interfaces;* Ishida, H.; Koenig, J.L., Eds.; Elsevier: New York, 1986; 143.
24. 24. A. A. Apostolov, S. Fakirov, B. Sezen, I. Bahar, and A. Kloczkowski, Polymer, 35, 5247 (1994).
25. Fakirov, S.; Evstatiev, M.; Friedrich, K. Nanostructured Polymer Composites from Polymer Blends: Morphology and Mechanical Properties. In *Handbook of Thermoplastic Polyesters, PET, PBT, PEN: Homopolymers, Copolymers, Blends and Composites*; Fakirov, S., Ed.; Wiley–VCH, Weinheim; September 2001
26. Keller, A.; Marchin, M.J. , J. Macromol, Sci. Phys. **1967**, B1, 41.
27. Khanna, Y.P.; Reimschussel, A.P. J. Appl. Polym. Sci. **1988**, 35, 2259.
28. Denchev, Z.; Kricheldorf, H.R.; Fakirov, S. Sequential Reordering in Condensation Copolymers. 6. Average Block Lengths in Poly(ethylene Terephthalate)–Polyamide 6 Copolymers as Revealed by NMR Spectroscopy. Macromol. Chem. Phys. **2001**, *202* (4), 574–586.
29. Paul, D.R.; Bucknall, C.B., Eds., *Polymer Blends, Vol. 2 Performance*; John Wiley and Sons, Inc., New York, 2000.
30. Gallagher, K.P.; Zhang, X.; Runt, J.P.; Huynh–ba, G.; Lin, J.S. Miscibility and Cocrystallization on Homopolymer-Segmented Block Copolymer Blends. Macromolecules **1993**, *26* (4), 588–596.

31. Apostolov, A.A.; Evstatiev, M.; Fakirov, S.; Kloczkowski, A.; Mark, J.E. Structures and Mechanical Properties of Zone-Drawn-Zone-Annealed Blends of cocrystallizing Poly(butylene Terephthalate) and a Poly (ether Ester). J. Appl. Polym. Sci. **1996**, *59* (11), 1667-1675.
32. Boneva, D.; Baltá Calleja F.J.; Fakirov, S.; Apostolov, A.A.; Krumova, M. Microhardness Under Strain. III. Microhardness Behavior During Stress-Induced Polymorphic Transition in Blends of Poly(butylene Terephthalate) and Its Block Copolymers. J. Appl. Polym. Sci. **1998**, *69* (11), 2271–2276.
33. Fakirov, S.; Apostolov, A.A.; Fakirov, C. Long Spacing in Polyblock Poly(ether Ester)s — Origin and Peculiarities. , Int. J. Polym. Mater. **1992**, *18* (1–2), 51–70.
34. Apostolov, A.A.; Bozvelieva, E.; Du Chesne, A.; Goranov, K.; Fakirov, S. Multiblock Poly(ether-ester-amide)s Based on Polyamide-6 and Poly(ethylene Glycol). 2. Effect of Composition and Soft-Segment Length on the Structure of Poly(ether-ester-amide)s as Revealed by X-ray Scattering. Macromol. Chem. **1993**, *194* (8), 2267–2277.
35. Peacock, J.A.; Hill, B.; Niel, E.; Barlow, C.Y. In *Composites Interfaces;* Ishida, H.; Koenig, J.L. Eds.; Elsevier: New York, 1986, 14.
36. Chen, E.J.H; Hsiao, B.S. The Effects of Transcrystalline Interphase in Advanced Polymer Composites. Polym. Eng. Sci. **1992**, *32* (4), 280–286.
37. Felix, J.M.; Gaterholm, P. Effect of Transcrystalline Morphology on Interfacial Adhesion in Cellulose/Polypropylene Composites. J. Mater. Sci. **1994**, *29*, 3043–3049.
38. Kumamaru, F.; Oono, T.; Kajivama, T.; Takayanagy, M. Interfacial Interaction Between Poly(*p*-phenylene Terephthalamide) Filament and Nylon 6 Matrix Crystallized from the Melt. Polym. Compos. **1983**, *4*, 141–148.
39. Klein, M.; Marom, G.; Wachtel, E. Microstructure of Nylon 66 Transcrystalline Layers in Carbon and Aramid Fibre Reinforced Composites. Polymer **1996**, *37* (24), 5493–5498.
40. Sapoundjieva, D.; Denchev, Z.; Evstatiev, M.; Fakirov, S.; Stribeck, N.; Stamm, M. Transcrystallization with Reorientation in Drawn PET/PA12 Blend as Revealed by WAXS from Synchrotron Radiation. J. Mater. Sci. **1999**, *34* (13), 3063–3066.
41. Groebe, A. In *Polymer Handbook*, 3rd Ed.; Bradrup, J., Immergut, E.H., Eds.; Wiley-Interscience: New York, 1989; Vol. 113, VI–111

Received March 12, 2001
Revised March 15, 2001
Accepted March 15, 2001